Journal of Applied Polymer Science

Characterization, Prediction, and Optimization of Flexural Properties of Vapor-Grown Carbon Nanofiber/Vinyl Ester Nanocomposites by Response Surface Modeling

Juhyeong Lee,[1] Sasan Nouranian,[2,3] Glenn W. Torres,[1] Thomas E. Lacy,[1] Hossein Toghiani,[2] Charles U. Pittman Jr.,[4] Janice L. DuBien[5]

[1]Department of Aerospace Engineering, Mississippi State University, Mississippi 39762
[2]The Dave C. Swalm School of Chemical Engineering, Mississippi State University, Mississippi 39762
[3]Center for Advanced Vehicular Systems (CAVS), Mississippi State University, Mississippi 39762
[4]Department of Chemistry, Mississippi State University, Mississippi 39762
[5]Department of Mathematics and Statistics, Mississippi State University, Mississippi 39762
Correspondence to: T. E. Lacy (E-mail: lacy@ae.msstate.edu)

ABSTRACT: A design of experiments and response surface modeling were performed to investigate the effects of formulation and processing factors on the flexural moduli and strengths of vapor-grown carbon nanofiber (VGCNF)/vinyl ester (VE) nanocomposites. VGCNF type (pristine, surface-oxidized), use of a dispersing agent (no, yes), mixing method (ultrasonication, high-shear mixing, and a combination of both), and VGCNF weight fraction (0.00, 0.25, 0.50, 0.75, and 1.00 parts per hundred parts resin (phr)) were selected as independent factors. Response surface models were developed to predict flexural moduli and strengths as a continuous function of VGCNF weight fraction. The use of surface-oxidized nanofibers, a dispersing agent, and high-shear mixing at 0.48 phr of VGCNF led to an average increase of 19% in the predicted flexural modulus over that of the neat VE. High-shear mixing with 0.60 phr of VGCNF resulted in a remarkable 49% increase in nanocomposite flexural strength relative to that of the neat VE. This article underscores the advantages of statistical design of experiments and response surface modeling in characterizing and optimizing polymer nanocomposites for automotive structural applications. Moreover, response surface models may be used to tailor the mechanical properties of nanocomposites over a range of anticipated operating environments. © 2013 Wiley Periodicals, Inc. J. Appl. Polym. Sci. 130: 2087–2099, 2013

KEYWORDS: composites; mechanical properties; thermosets; properties and characterization

Received 1 February 2013; accepted 9 April 2013; Published online 15 May 2013
DOI: 10.1002/app.39380

INTRODUCTION

The increasing demand for light-weight and low-cost structural parts to achieve improved vehicle fuel efficiency is one key motivation for the rapid development of advanced automotive materials. Nano-enhanced thermoplastic and thermoset polymer composites[1,2] have emerged as an attractive class of composite materials with promising mechanical properties.[3] Nanoreinforcements typically have exceptionally high surface-area-to-volume ratios that permit improved load transfer and subsequently increased bulk mechanical properties with very low nanoreinforcement weight fractions. However, several issues hinder the optimal fabrication and utilization of polymer nanocomposites, i.e., poor nanoreinforcement dispersion, alignment, and interfacial adhesion.[4,5] Jordan et al.[6] reviewed recent experimental attempts at improving these issues. Better nanoreinforcement dispersion has been achieved through aggressive mixing techniques, such as ultrasonication,[7] ball milling,[8] three-roll milling,[9] thermo-kinetic mixing,[10] chaotic mixing,[11] and internal mixing.[12] Chemicals have been added to the resin formulation to aid in nanoreinforcement dispersion.[13–15] Improved interfacial adhesion has been realized through functionalization of nanoreinforcement surfaces.[16,17] The majority of these efforts have involved single-factor studies, which cannot account for interactions between fabrication/processing factors and their combined effects on the nanocomposite mechanical properties. Understanding formulation and processing factor interactions is especially important if large-scale industrial fabrication of optimized nanocomposite systems for different applications is desired.

Vapor-grown carbon nanofibers (VGCNFs) are attractive nanoreinforcements for use in thermoplastic and thermoset

Table I. Experimental Design Factors and their Respective Levels and Types

Design factor and designation	Levels					Type
	1	2	3	4	5	
VGCNF[a] type (A)	Pristine	Oxidized	–	–	–	Qualitative
Use of a dispersing agent (B)	No	Yes	–	–	–	Qualitative
Mixing method (C)	US[b]	HS[c]	HS/US[d]	–	–	Qualitative
VGCNF weight fraction (D)	0.00[e]	0.25	0.50	0.75	1.00	Quantitative

[a] Vapor-grown carbon nanofiber.

[b] Ultrasonication.

[c] High-shear mixing.

[d] Coupled high-shear mixing and ultrasonication.

[e] Neat resin used as control. The treatment combinations involving 0.00 phr VGCNF are simply neat resin specimens all prepared the same way irrespective of the other factor levels.

matrices.[18] Vinyl esters (VEs)[19] are widely used commodity resins with good mechanical and corrosion properties, superior to unsaturated polyesters. VGCNF/VE nanocomposites could be utilized as nano-enhanced matrices in laminated composites for a wide range of industrial applications.[20] Relatively few reports exist that address the mechanical characterization of these nanocomposites. Plaseied et al.[21,22] measured and modeled the tensile, flexure, and creep behavior of VGCNF/VE nanocomposites. They reported a 6% increase in the flexural modulus and strength of the VE through the addition of 1 wt % functionalized VGCNFs.[21] Hutchins et al.[23] investigated the compressive high-strain-rate behavior of VGCNF/VE nanocomposites using split-Hopkinson bar testing. Nouranian et al.[24,25] used a full-factorial design of experiments and response surface modeling to predict the viscoelastic responses (storage and loss moduli) of VGCNF/VE nanocomposites over a wide range of operating temperatures. They reported an average increase of 20% in the storage modulus relative to the neat VE by incorporating less than 0.50 parts of VGNCF in 100 parts of VE resin (0.50 phr). Torres et al.[26] used a central composite design to predict and optimize Izod impact strengths of VGCNF/VE nanocomposites. They demonstrated an 18% increase in the nanocomposite impact strength relative to that of the neat VE by incorporating only 0.170 phr of VGCNFs in VE.

This article investigates the combined effect of various formulation and processing factors on the flexural moduli and strengths of VGCNF/VE nanocomposites in the framework of a robust experimental design.[27] One objective is to provide a statistically reliable and reproducible method to fabricate these materials with a focus on the prediction and optimization of their mechanical performance through response surface modeling.[28] Such modeling approaches have previously been used for the optimization of composite material properties.[29–33] Response surface models (RSMs) establish functional relationships between independent variables and the response that can lead to insight into the physical behavior. These predictive models enable the tailoring of nanocomposites for different applications through selective manipulation of relevant design factors. In addition, these models may be efficiently used to guide the development of physics-based models.

MATERIALS AND METHODS

Design of Experiments

A statistical design of experiments was used to characterize the VGCNF/VE nanocomposite flexural moduli and strengths for a combination of three qualitative (discrete) and one quantitative (continuous) formulation and processing factors. These factors, their designations, and levels are shown in Table I. The selected factors and their levels encompass some of the state-of-the-art mechanical and chemical methods to effectively resolve the nanoreinforcement dispersion and interfacial adhesion issues in polymer nanocomposites. Hence, no screening experiments were performed to arrive at the current list of design factors and their levels. The maximum level for VGCNF weight fraction (1.00 phr) was selected to limit the viscosity of the VGCNF/resin blend. For given mixing techniques, VGCNF weight fractions in excess of 1.00 phr led to high viscosities that made it difficult to process the blends.

A general mixed-level full factorial design was used to generate all possible factorial arrangements of the factor levels in Table I into a total of 60 "treatment combinations." A treatment combination ("run") is a sequence of various factor levels in a given experimental trial. The flexural modulus and strength were selected as responses, i.e., outputs of the process or dependent variables. The flexural specimens were prepared from a single batch of VGCNF/VE blend for each treatment combination in Table I. The analysis of the data was performed in SAS® 9.2 statistical analysis software.

Materials and Specimen Preparation

An infusion-class VE resin (Ashland Chemical, Derakane 441-400) with 33 wt % styrene and an average molecular weight of 690 g/mol[34] was selected for the matrix because of its superior thermal properties and corrosion resistance. Pristine VGCNFs (PR-24-XT-LHT) and oxidized VGCNFs (PR-24-XT-LHT-OX) were both purchased from Applied Sciences, Inc. and were used as-received without further modification. PR-24-XT-LHT has an average diameter of 150 nm, a surface area of 35–45 m^2/g, and a dispersive surface energy of 155 mJ/m^2 based on the manufacturer's datasheet. Similar data for the oxidized version has not been disclosed by the manufacturer. While the nature of the

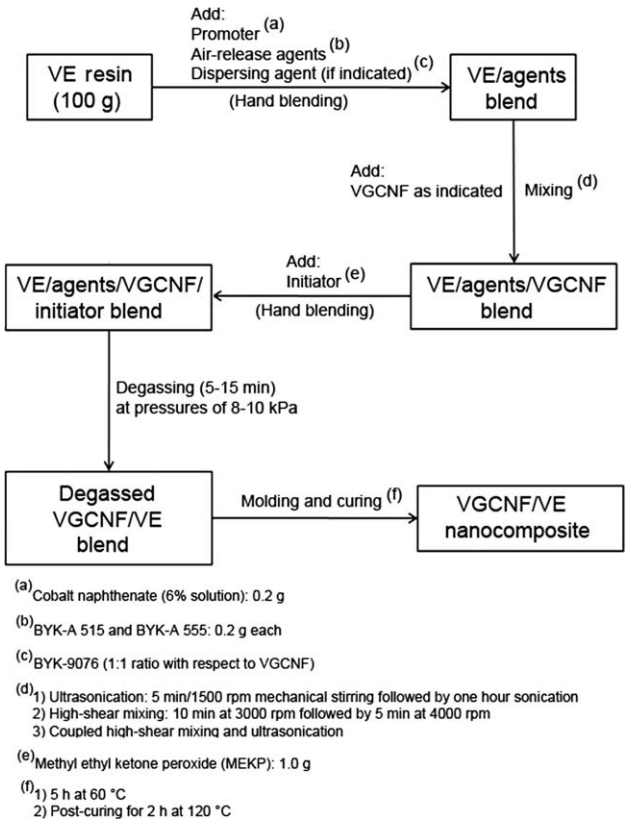

Figure 1. The VGCNF/VE specimen fabrication scheme.

functional groups introduced on the surface of the oxidized nanofibers is proprietary, they may include phenolic hydroxyl groups, lactones, carboxylic acids, and ethers (where the ether oxygen atoms are ring atoms), ketones and quinones.[17,35] Such functional groups may improve nanofiber–matrix adhesion by interacting with the oxygen-containing polar groups within the VE molecules. Changes in VGCNF mechanical properties or surface areas are highly resistant to oxidative treatment,[17] so the effect of nanofiber oxidation on composite properties results only from changes in the nanofiber to matrix adhesion. A 6 wt% solution of cobalt naphthenate in styrene (North American Composites) in combination with methyl ethyl ketone peroxide (MEKP) (US Composites) were used as the promoter and free radical initiator to cure the resin, respectively. BYK-A 515 and BYK-A 555 (BYK Chemie GmbH) were used as air release additives to minimize void formation in the final cured nanocomposite. BYK-9076 (BYK Chemie GmbH) was selected as a dispersing agent (DA) for VGCNFs. BYK-9076 is a proprietary copolymer alkylammonium salt acting as a surface-active agent that has been used for various nanocomposite formulations.[15,16,24] The optimal ratio of the amount of DA to the amount of VGCNFs was 1:1 by weight, based on the recommendations by the supplier. The flexural specimens were fabricated according to the formulation and protocol reported previously.[24] A schematic of the protocol is given in Figure 1.

Flexural Testing

Quasi-static four-point bending tests (ASTM D 6272) were performed on two nanocomposite specimens prepared from each treatment combination using an Instron 5869 Universal Testing Machine with a 5-kN load cell. A schematic of a four-point bending test specimen (Support span, $L = 60$ mm; width, $b = 12.7$ mm; thickness, $d = 3$ mm) with a support span to load span ratio of 2:1 is shown in Figure 2. A standard support span-to-width ratio of $L/b = 14$ was used to avoid possible transverse shear stress effects. The bulk flexural modulus and flexural strength for a specimen is determined by

$$E = 0.17\frac{mL^3}{bd^3}, \quad (1)$$

$$S = \frac{3PL}{4bd^2}, \quad (2)$$

where E is the flexural modulus, S is the flexural strength, and P, L, b, d, and m are the failure load, support span, specimen width, specimen thickness, and slope of the midpoint load–deflection curve, respectively.

The top and bottom surfaces of each specimen were polished to remove surface defects. To determine the average dimensions (thickness and width) after polishing, each flexural specimen was measured at 10 separate locations. The crosshead displacement rate was set to provide a strain rate of 0.0002/s.

RESULTS AND DESCUSSION

The flexural moduli and strengths obtained from two separate specimens per each treatment combination were averaged for use in the statistical analysis. The treatment combinations (runs) and their respective responses (flexural moduli and strengths) are shown in Table AI. The measured flexural moduli fell in the range $E = 2.59$–3.69 GPa with an average standard deviation of 100–200 MPa. The measured flexural strengths were in the range $S = 38.1$–117.1 MPa with an average standard deviation of 5–10 MPa. These averages were calculated from individual standard deviations for each treatment combination response.

Statistical Analysis of the Flexural Moduli

Analysis of Variance. As the test specimens were prepared from a single batch of VGCNF/VE blend (one replicate of each treatment combination in Table AI), no experimental error could be calculated for the Analysis of Variance (ANOVA)[36] in this article. Therefore, it was assumed that three- and four-factor interactions were negligible and the experimental error was constructed from these higher order interactions.[37] Hence, the

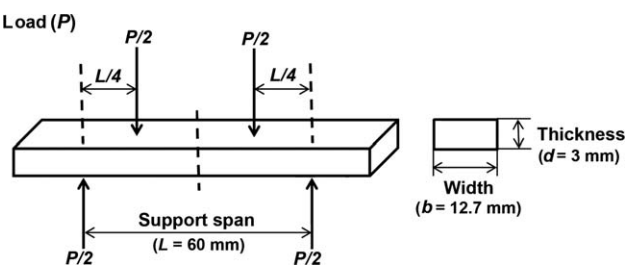

Figure 2. Test specimen geometry for the four-point bending test.

Table II. Analysis of Variance (ANOVA) Results for the Flexural Modulus Data

Source of variation	Degrees of freedom	Sum of squares	Mean square	*F*-value	*P*-value[a]
Model	29	2.63	0.091	4.55	<0.0001
A: VGCNF Type	1	0.01	0.014	0.72	0.4037
B: Use of dispersing agent	1	0.11	0.11	5.39	0.0272[b]
C: Mixing method	2	0.80	0.40	20.14	<0.0001[b]
D: VGCNF weight fraction	4	0.44	0.11	5.54	0.0018[b]
A × B	1	0.0060	0.0060	0.29	0.5970
A × C	2	0.44	0.22	10.91	0.0003
A × D	4	0.27	0.068	3.38	0.0213
B × C	2	0.091	0.045	2.27	0.1205
B × D	4	0.22	0.055	2.75	0.0464
C × D	8	0.24	0.030	1.51	0.1940
Error	30	0.60	0.020	-	-
Total (Corrected)	59	3.23	-	-	-
	Other model statistics				
Mean: 3.21		R^2: 0.82			
Coefficient of variation: 4.40%		Standard deviation: 0.14			

[a] Observed significance level. *P*-values < 0.05 are considered significant in this analysis.

[b] These factors are involved in higher order interactions.

Note: The underlined two-factor interactions are significant.

model selected for the ANOVA had all four main effects pertaining to factors A (VGCNF type), B (use of a DA), C (mixing method), and D (VGCNF weight fraction) and their two-factor interactions (A × B, A × C, etc.). All sources of variation for the flexural moduli are summarized in Table II, including their associated *F*- and *P*-values that are used for the ordered *F*-tests to determine significant factorial effects.[36] The factorial effects with a *P*-value *less* than a desired significance level ($\alpha = 0.05$ in this case) are considered to be significant.

In Table II, three higher order interaction effects with *P*-values < 0.05 are significant for the flexural modulus: (1) interaction between the VGCNF type and the mixing method (A × C); (2) interaction between the VGCNF type and the VGCNF weight fraction (A × D); and (3) interaction between the use of a DA and the VGCNF weight fraction (B × D). The VGCNF weight fraction (D) is the *only* quantitative (continuous) factor involved in the significant A × D and B × D interactions. Therefore, it was used as an independent variable in the generation of all RSMs. As qualitative factors A (VGCNF Type) and B (use of a DA) each have two levels (Table I), four RSMs ($2 \times 2 = 4$) can be generated with the quantitative factor D as the independent variable. However, the VGCNF type (A) is also involved in the significant A × C interaction, with the qualitative factor C (mixing method) having three distinct levels (Table I). As a consequence, the possible number of RSMs for the flexural modulus is further increased to 12 ($2 \times 2 \times 3 = 12$, where the numbers on the left-hand side of the equality denote factor levels).

Fisher's Least Significant Difference Tests. Fisher's protected least significant difference (LSD) tests[38] were performed on the mean flexural moduli associated with the A × C interaction (the only significant interaction not involving the quantitative factor D) to *reduce* the total number of required RSMs. In Table III, the mean flexural modulus values associated with six level combinations of factors A (VGCNF type) and C (mixing method) are listed in descending order. In Fisher's method, an LSD value is calculated[28] and *t*-tests are run on the differences between all

Table III. Least Significant Difference (LSD) Test Results for the Interaction Between VGCNF Type and Mixing Method (A × C)

t-grouping	Least squares mean values for the flexural modulus (GPa)	VGCNF type (A)	Mixing method (C)
X[a]	3.49	Oxidized	HS[b]
Y	3.25	Pristine	HS
Y			
Y	3.18	Oxidized	HS/US[c]
Y			
Y	3.18	Pristine	US[d]
Y			
Y	3.16	Pristine	HS/US
Z	3.01	Oxidized	US

[a] Least squares means with the same letters are not significantly different from each other.

[b] High-shear mixing.

[c] Coupled high-shear mixing and ultrasonication.

[d] Ultrasonication.

pairs of the mean values. If the calculated *t*-value is greater than the LSD value, the difference is deemed significant. The results are presented in a standard graphical format, where mean flexural moduli are designated with arbitrary letters (X, Y, and Z in this case) in a "*t*-grouping" column (Table III). In comparing any two mean flexural modulus values, the difference is statistically significant if and only if the letters associated with them in the *t*-grouping column are different. For example, the combination oxidized VGCNF/high-shear mixing (designated as HS) has letter "X" in its *t*-grouping column (Table III). Therefore, its associated mean flexural modulus is significantly different from the mean flexural modulus for the combination pristine VGCNF/ultrasonication (designated as US), which has letter "Y" in its *t*-grouping column. In Table III, all three A × C combinations (rows) for specimens containing oxidized VGCNFs, i.e., oxidized VGCNF/HS versus oxidized VGCNF/US versus oxidized VGCNF/coupled HS/US, have different designated letters in the *t*-grouping column and, hence, yield significant differences in their mean flexural modulus values. This is not true for the three A × C combinations for specimens containing pristine VGCNFs (all have letter "Y" in the *t*-grouping column). This suggests that the mixing method (factor C) only affects the mean flexural modulus of the nanocomposite specimens containing oxidized VGCNFs. Therefore, three data combinations involving oxidized VGCNFs (one for each mixing method) and one grouped data combination involving pristine VGCNFs are selected for response surface modeling purposes. If one considers the significant A × D interaction (Table II), which is the basis for generating RSMs together with the significant B × D interaction (both involve the quantitative factor D), the number of RSMs for the flexural modulus could thereby be reduced to eight ($2 \times 4 = 8$, where number 2 denotes the number of levels for factor B and number 4 denotes the reduced number of combinations for the A × C interaction). To further simplify the analyses, only the data set associated with the oxidized VGCNF/HS mixing combination (yielding the *highest* mean flexural modulus in the first row of Table III) was selected for response surface modeling among the A × C combinations involving oxidized VGCNFs. This was consistent with the objective of this article to maximize the flexural modulus. Hence, the total number of requisite RSMs was reduced to four, i.e., RSMs for the mean flexural moduli associated with pristine VGCNF/no DA (designated as E_1), pristine VGCNF/DA (E_2), oxidized VGCNF/no DA/HS mixing (E_3), and oxidized VGCNF/DA/HS mixing combinations (E_4).

Flexural Modulus Response Surface Modeling. In general, the RSM giving the flexural moduli (E) as a function of VGCNF weight fractions (D) can be written as follows:

$$E = \beta_0 + \sum_{j=1}^{a} \beta_j D^j, \tag{3}$$

where β_0 is the intercept, β_j's are model parameters, and a is the order of the polynomial. Several polynomial fits (linear, quadratic, cubic, etc.) were considered for the data points. Nanocomposite mechanical properties often increase up to a local maximum with increasing amounts of nanoreinforcements.[24,25] Further increase in the amount of nanoreinforcements, however, can result in a decrease in the properties. Quadratic and cubic RSMs were employed in this article as they can easily account for the curvature in the flexural moduli and strengths associated with changes in the amount of VGCNFs. Cubic fits gave highest R^2 (amount of variation explained by the model) and adjusted R^2 values. The highest R^2 values are typically sought for an adequate fit. Regression analysis results are summarized in Table AII. The final predictive RSMs for the nanocomposite specimens containing pristine VGCNFs are given below. Note that for these specimens, the mean flexural modulus is insensitive to the mixing method:

$$E_1 = 3.12 - 1.63D + 5.26D^2 - 3.62D^3, \tag{4}$$

$$E_2 = 3.13 + 1.86D - 4.42D^2 + 2.70D^3, \tag{5}$$

where E_1 and E_2 correspond to pristine VGCNF/no DA and pristine VGCNF/DA combinations, respectively. Similarly, the final predictive RSMs for the specimens containing oxidized VGCNFs are given below. For specimens containing oxidized VGCNFs, the mean flexural modulus is significantly affected by the choice of mixing method. Here, however, only the RSMs associated with the HS mixing method, yielding the highest mean flexural modulus, are considered.

$$E_3 = 3.11 + 1.27D - 1.17D^2 + 0.43D^3, \tag{6}$$

$$E_4 = 3.12 + 2.95D - 4.70D^2 + 2.26D^3, \tag{7}$$

where E_3 and E_4 correspond to oxidized VGCNF/no DA/HS mixing and oxidized VGCNF/DA/HS mixing combinations, respectively.

The amounts of variation in the data explained by eqs. (4)–(7) are 63, 34, 99, and 96%, respectively (see the R^2 values in Table AII). The four RSMs are plotted and compared in Figures 3(a–c). In these figures, the actual mean flexural modulus values and their respective standard deviations (error bars) are also presented.

Observations and Physical Insights. The predicted flexural modulus exhibited a steady increase with increasing VGCNF weight fraction for the nanocomposite specimens containing oxidized VGCNFs and no DA [Figure 3(a)]. These predicted flexural moduli were higher for the nanocomposites composed of oxidized VGCNFs than for those containing pristine VGCNFs. The nanocomposite specimens prepared with pristine VGCNFs and no DA (E_3) showed flexural moduli at low VGCNF weight fractions ($D <$ 0.50 phr) *below* that of the neat VE [Figure 3(a)]. At higher VGCNF weight fractions, a slight improvement in the predicted flexural modulus was observed [Figure 3(a)]. By incorporating a DA in the nanocomposite formulation, an increase in the predicted flexural modulus was observed for nanocomposite specimens containing $D = 0.48$ phr of oxidized VGCNFs (up to a maximum of $E = 3.71$ GPa, which is 19% greater than that of the neat VE) [Table AII and Figure 3(b)]. At low pristine VGCNF weight fractions ($D <$ 0.50 phr),

Applied Polymer SCIENCE

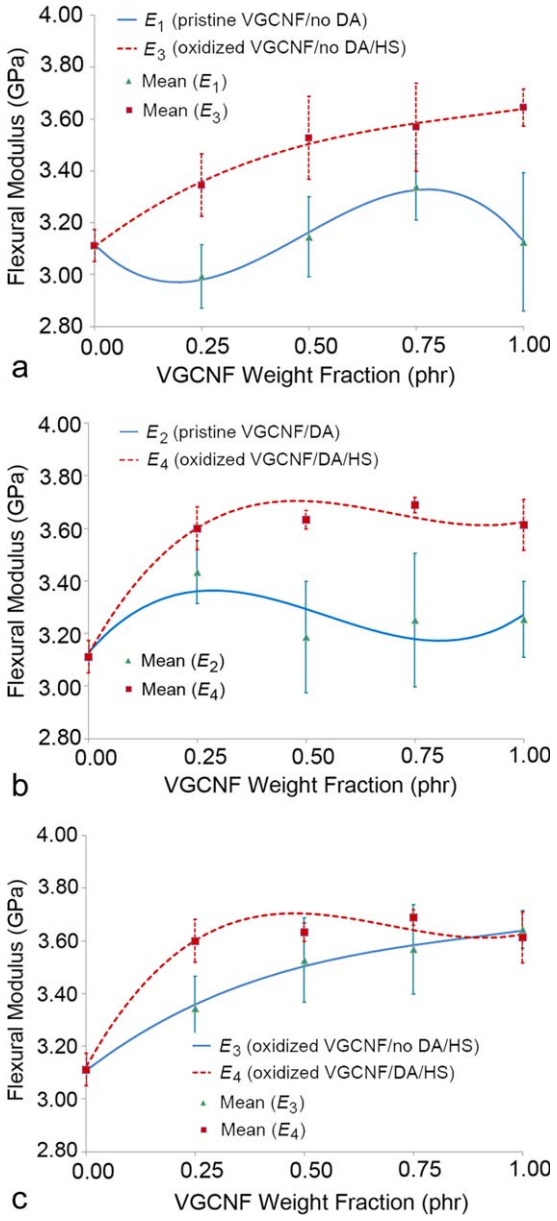

Figure 3. a) Flexural modulus response surface plots of (a) E_1 (pristine VGCNF/no DA) and E_3 (oxidized VGCNF/no DA/HS), (b) E_2 (pristine VGCNF/DA) and E_4 (oxidized VGCNF/DA/HS), and (c) E_3 (oxidized VGCNF/no DA/HS) and E_4 (oxidized VGCNF/DA/HS). The actual mean flexural modulus data are also presented with error bars. HS and DA denote high-shear mixing and DA, respectively. [Color figure can be viewed in the online issue, which is available at wileyonlinelibrary.com.]

using a DA improved the nanocomposite flexural moduli over that of the neat VE [Figure 3(b)] with a maximum flexural modulus of $E = 3.36$ GPa (8% increase over that of the neat VE) obtained at $D = 0.29$ phr of pristine VGCNFs [Table AII and Figure 3(b)]. Furthermore, nanocomposite specimens prepared using oxidized VGCNFs, DA, and HS mixing display the least scatter in the measured flexural moduli [Figures 3(b,3c)].

Surface oxidation of carbon nanofibers significantly increases nanocomposite flexural moduli. This is evident by contrasting the two RSMs associated with oxidized VGCNFs in Figures 3(a,b) ($E_3$and E_4) with those of the pristine VGCNFs (E_1 and E_2). Effective load transfer from the matrix to carbon nanofibers requires strong interfacial adhesion,[5] which may be improved by surface oxidation of VGCNFs. Another possible factor contributing to the improved flexural modulus in oxidized VGCNF/VE nanocomposites is reduced nanofiber agglomeration. Strong van der Waals forces and mechanical interlocking between individual nanofibers often leads to agglomerates with the overall effect of lowering the nanocomposite flexural modulus. Nanofibers locked within the agglomerates do not contribute to the material's stiffness. This may be more profound in the case of pristine nanofibers, which have more tightly interlocked nanofibers within their agglomerates and where agglomeration is aggravated by the relatively large surface energies of the individual nanofibers. In contrast, oxygenated surface functions reduce surface energy and promote attractive interactions (wetting) with polar oxygen-containing functional groups present in the resin.[39] This wetting could promote nanofiber dispersion during mixing leading to fewer and smaller nanofiber agglomerates in the cured nanocomposites.

Use of a DA, like employing nanofiber surface oxidation, facilitates nanofiber de-agglomeration by reducing nanofiber–nanofiber attractive interactions. The DA has terminal polar groups, which associate with polar groups on the oxidized nanofiber surfaces and act synergistically with the oxidized VGCNFs to promote better nanofiber dispersion. This leads to higher flexural moduli [Figure 3(c)]. A DA also sharply reduces VGCNF/VE blend viscosities. This is very important for processing as the viscosities of VGCNF/VE blends rapidly increase as the VGCNF weight fraction increases from 0.00 to 1.00 phr. At still higher VGCNF weight fractions (D $\geq$ 2.00 phr), the blend has a paste-like consistency that makes it impossible to mold or to infuse into continuous fiber preforms. As a comparison, Sudduth[40] reported a dramatic viscosity increase as the volume fractions of differently shaped pigment particles, especially those with high aspect ratios, increased in pigment suspensions.

VGCNF de-agglomeration is mainly achieved through mechanical shearing during nanofiber/resin blend mixing. Shearing disentangles the nested nanofibers providing a larger surface area for nanofiber–matrix interactions, thereby benefitting the mechanical properties. Mixing is therefore a crucial step and insufficient or excessive mixing can have undesirable effects on the mechanical properties. The flexural moduli of nanocomposites containing pristine nanofibers are not sensitive to the variations in mixing employed in this article. This observation is confirmed by the LSD test results in Table III, where the mean flexural modulus associated with A $\times$ C combinations involving pristine VGCNFs are not significantly different from each other. Conversely, the mean flexural modulus improved in oxidized VGCNF samples by varying the mixing method (Table III). US (ultrasonication) mixing led to the smallest mean flexural modulus for the oxidized VGCNFs, whereas HS mixing resulted in the largest. The mean flexural modulus deteriorates when the mixing is switched from HS to coupled HS/US mixing (Table III). Excessive mixing (in this case coupled HS/US mixing) may cause nanofiber breakage leading to a decreased nanofiber

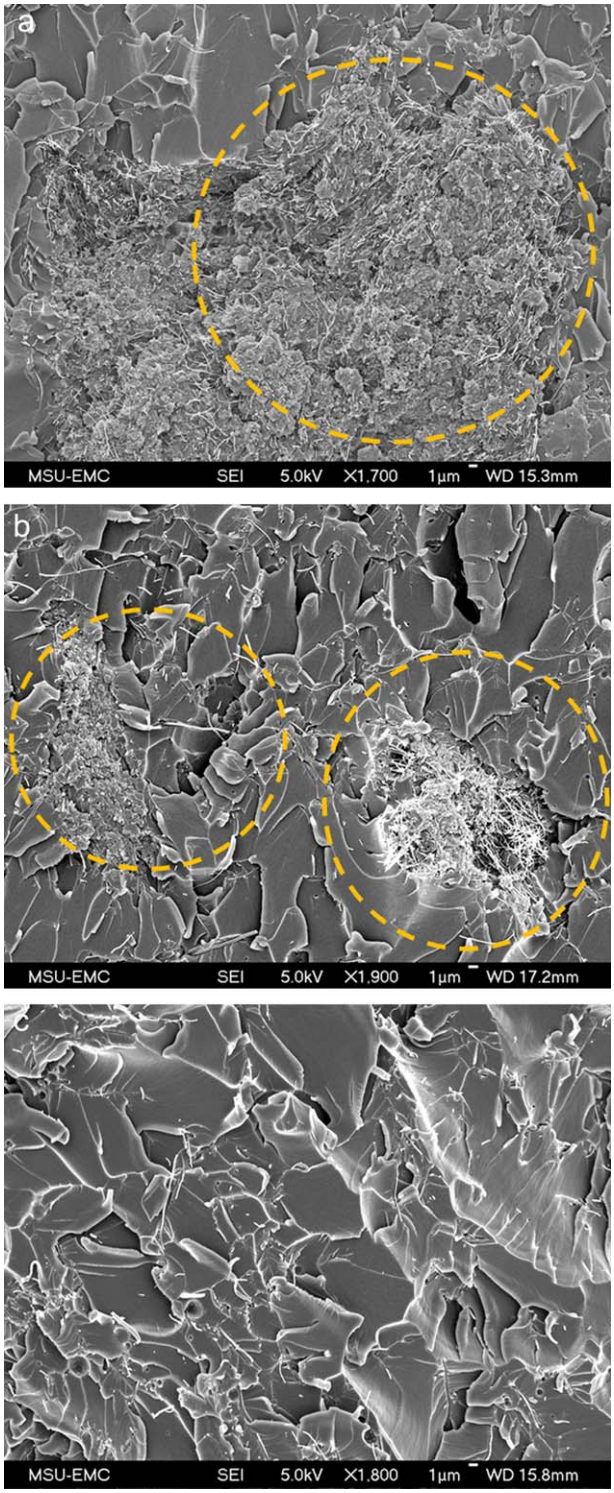

Figure 4. Scanning electron micrographs of the fracture surfaces of three VGCNF/VE nanocomposites: (a) 1.00 phr pristine VGCNF without DA prepared by ultrasonication, where a large nanofiber agglomerate can be seen, (b) 1.00 phr oxidized VGCNF without DA prepared using high-shear mixing, where smaller size agglomerates are observed, and (c) 1.00 phr oxidized VGCNF with DA prepared using high-shear mixing, where a uniform distribution of nanofibers can be seen. [Color figure can be viewed in the online issue, which is available at wileyonlinelibrary.com.]

aspect ratio distribution. Reducing nanofiber aspect ratios below 50 has been predicted to detrimentally affect nanocomposite moduli.[41] Figure 4 contains representative scanning electron microscopy images for three different VGCNF/VE nanocomposites at the same VGCNF weight fraction (1.00 phr) that illustrate typical microstructural features resulting from the use of different mixing techniques in specimen preparation. In general, US mixing does not break up large nanofiber agglomerates [Figure 4(a)], whereas HS mixing tends to reduce the agglomerate sizes drastically [Figure 4(b)]. Use of a DA in combination with HS mixing can further reduce the size and number of agglomerates yielding more uniformly dispersed nanofibers in the cured resin [Figure 4(c)].

Statistical Analysis of Flexural Strengths

Analysis of Variance (ANOVA). The ANOVA model for flexural strength was similar to that employed for the flexural modulus where all four main effects of the factors and two-factor interactions were considered in the model. Higher three- and four-factor interactions were assumed negligible to construct the error term for the ANOVA. This assumption was reasonable as only one batch was prepared for each run in Table AI. All sources of variation in the flexural strengths data are shown in Table IV. Two interactions were considered significant (P-value < 0.05): (1) the interaction between the use of a DA and the mixing method ($B \times C$); and (2) the interaction between the mixing method and the VGCNF weight fraction ($C \times D$). The factors C (mixing method) and D (VGCNF weight fraction), which also have P-values less than 0.05, are involved in higher order interactions. Therefore, their main effects were not analyzed separately. The quantitative factor D was used as the independent variable in all RSMs similar to the case for the flexural modulus. Factor B (use of a DA) has two levels and factor C (mixing method) has three levels (Table I). This means that a significant $B \times C$ interaction leads to six ($2 \times 3 = 6$) possible RSMs for the flexural strength.

Fisher's LSD Tests. Fisher's LSD tests were conducted on the mean flexural strength values associated with the six factor level combinations pertaining to the $B \times C$ interaction in Table V. This was done to reduce the total number of required RSMs for the flexural strength, similar to the approach used for the flexural modulus. In Table V, the results of the t-tests are summarized using designated letters in the t-grouping column. This time, some combinations have more than one letter (W, X, Y, or Z) associated with their mean flexural strength values in their t-grouping column. In interpreting the differences between pairs of mean flexural strength values, those with at least one common letter in their t-grouping column are not significantly different from each other. The information in Table V is only used to identify those mixing methods that are sensitive to the use of a DA, thereby aiding in the determination of required RSMs. On this basis, the combinations DA/US mixing and no DA/US mixing were the only $B \times C$ combinations deemed significantly different from each other (designated by letters Y and Z in their respective rows in the t-grouping column). Therefore, the total number of RSMs was reduced from six (taking into account all $B \times C$ combinations) to four (including only the significant $B \times C$ combinations in Table V).

Table IV. Analysis of Variance (ANOVA) Results for the Flexural Strength Data

Source of variation	Degrees of freedom	Sum of squares	Mean square	*F*-value	*P*-value[a]
Model	29	17,783.13	613.21	5.69	<0.0001
A: VGCNF Type	1	252.51	252.51	2.34	0.1363
B: Use of dispersing agent	1	440.75	440.75	4.09	0.0521
C: Mixing method	2	7504.19	3752.10	34.82	<0.0001[b]
D: VGCNF weight fraction	4	2778.99	694.75	6.45	0.0007[b]
A × B	1	3.00	3.00	0.03	0.8685
A × C	2	11.39	5.70	0.05	0.9486
A × D	4	435.90	108.98	1.01	0.4173
B × C	2	1727.61	863.80	8.02	0.0016
B × D	4	831.52	207.88	1.93	0.1314
C × D	8	3797.26	474.66	4.40	0.0013
Error	30	3233.15	107.77	-	-
Total (Corrected)	59	21,016.28	-	-	-
	Other model statistics				
Mean: 78.6			R^2: 0.85		
Coefficient of variation: 13.2%			Standard deviation: 10.4		

[a] Observed significance level. *P*-values <0.05 are considered significant in this analysis.

[b] These factors are involved in higher order interactions.

Note: The underlined two-factor interactions are significant.

Flexural Strength Response Surface Modeling. The final set of RSMs for the mean flexural strengths were associated with no DA/US mixing (S_1), DA/US mixing (S_2), HS mixing (S_3), and coupled HS/US mixing combinations (S_4). Polynomial fits giving higher R^2 and adjusted R^2 values were selected. The regression analysis results are summarized in Table AIII. The final RSMs below give the flexural strength (S) as a function of VGCNF weight fraction (D) for the US mixing combinations. Note that the flexural strength is sensitive to the use of a DA in the formulation of the nanocomposite specimens prepared using the US mixing method.

$$S_1 = 67.3 - 183.9D + 437.0D^2 - 273.0D^3, \quad (8)$$

$$S_2 = 66.9 - 221.3D + 678.8D^2 - 443.4D^3, \quad (9)$$

where S_1 and S_2 correspond to no DA/US mixing and DA/US mixing combinations, respectively. The final RSMs for the HS and coupled HS/US mixing methods are given below. In these cases, the DA does not affect the mean flexural strength significantly.

$$S_3 = 69.5 + 104.6D - 87.8D^2, \quad (10)$$

$$S_4 = 68.3 + 92.2D - 166.8D^2 + 102.5D^3, \quad (11)$$

where S_3 and S_4 correspond to the HS and coupled HS/US mixing combinations, respectively. These models (eqs. 8–11) describe 78, 77, 71, and 39% of the variations in the data, respectively (see the R^2 values in Table AIII). The RSMs are plotted and compared in Figures 5(a,b), where the actual mean flexural strength values and their respective standard deviations (error bars) are also shown.

Observations and Physical Insights. The predicted flexural strengths were markedly different for the nanocomposites prepared by the three mixing methods [Figure 5(a)]. Furthermore, only the flexural strengths of the nanocomposite specimens

Table V. Least Significant Difference (LSD) Test Results for the Interaction Between the Use of Dispersing Agent and Mixing Method (B × C)

t-grouping	Least squares mean values for the flexural strength (MPa)	Use of a dispersing agent (B)	Mixing method (C)
W[a]	91.9	Yes	HS[b]
W			
X W	87.9	No	HS/US[c]
X W			
X W	85.9	No	HS
X			
X Y	79.9	Yes	HS/US
Y			
Y	72.2	Yes	US[d]
Z	53.9	No	US

[a] Least squares means with the same letters are not significantly different.

[b] High-shear mixing.

[c] Coupled high-shear mixing and ultrasonication.

[d] Ultrasonication.

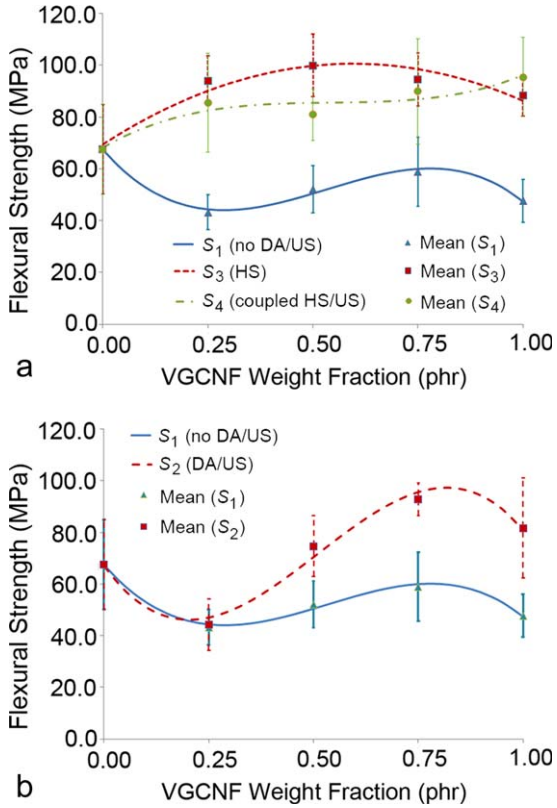

Figure 5. Flexural strength response surface plots of (a) S_1 (no DA/US), S_3 (HS), and S_4 (coupled HS/US), and (b) S_1 (no DA/US) and S_2 (DA/US). The actual mean flexural strength data are also presented with error bars. US, HS, and DA denote ultrasonication, high-shear mixing, and DA, respectively. [Color figure can be viewed in the online issue, which is available at wileyonlinelibrary.com.]

prepared by the US mixing method were sensitive to the use of a DA in their formulation [Figure 5(b)]. The predicted flexural strengths were not affected by the VGCNF type. Nanocomposite strengths are likely associated with the size distribution of VGCNF agglomerates more than the nanofiber–matrix interfacial adhesion. Hence, factors leading to a more uniform dispersion of VGCNFs in the resin (i.e., mixing and the use of a DA) will have a greater influence on the cured nanocomposite strengths. HS mixing yielded the highest nanocomposite flexural strength $S \approx 101$ MPa at a VGCNF weight fraction $D = 0.60$ phr [Table AIII and Figure 5(a)]. *This is a remarkable 49% increase in the nanocomposite flexural strength over that of the neat VE for a tiny VGCNF weight fraction.* At higher VGCNF weight fractions ($D > 0.60$ phr), the flexural strength dropped slightly [Figure 5(a)].

US mixing resulted in markedly lower flexural strengths versus that of the neat VE (10–40% decrease) when no DA was used in the nanocomposite formulation [Figure 5(a)]. In contrast, when the DA was present, the nanocomposite flexural strengths improved over that of neat cured VE resin at VGCNF weight fractions $D > 0.50$ phr. Here, the DA better improves the flexural strengths at higher VGCNF weight fractions when combined with US mixing. A combination of HS and US mixing [coupled HS/US mixing in Figure 5(a)] results in an intermediate improvement in the nanocomposite flexural strengths. This trend suggests that the nanocomposite flexural strengths can be maximized with optimal mixing.

Strength is dominated by a variety of failure mechanisms such as crack nucleation and propagation. In VGCNF/VE nanocomposites, nanofiber agglomerations act as stress concentrators and crack nucleation sites. Crack nucleation, growth, and coalescence will ultimately lead to the material's failure. Nanofibers can act as crack deflectors forcing very small cracks to follow a more tortuous path or cause crack bridging.[42] The more cracks that are deflected, the higher the material's toughness and flexural strength will be. Uniformly distributed nanofibers with a minimum of agglomerates will lead to higher nanocomposite flexural strength. Agglomerates with dimensions that are large in comparison to typical nanofiber lengths effectively serve as defects whose growth cannot be arrested by nearby well-dispersed nanofibers. This trend is observed for the VGCNF/VE specimens prepared using HS mixing. It is anticipated that more aggressive mixing in the case of coupled HS/US mixing leads to an excessive chopping of nanofibers and a reduced average nanofiber aspect ratio. Hence, the nanocomposite small crack deflection capability may not be as effective as the case for nanofibers with higher aspect ratios.

Nanocomposite Optimization

Higher flexural modulus and strength are both desired in structural applications. The RSMs developed here for the flexural moduli and strengths of VGCNF/VE nanocomposites can be used to optimize both properties within the design space considered in this article. For example, oxidized VGCNFs yield the highest flexural modulus, whereas the VGCNF type has no significant effect on the flexural strength. This suggests that oxidized nanofibers should be used to maximize flexural moduli and strengths. Similarly, the use of a DA is recommended as it has a significant positive effect on the flexural modulus, but no significant effect on the flexural strength, except for the specimens prepared using the US mixing method. Moreover, use of a DA significantly reduces the VGCNF/VE blend viscosity. Finally, HS mixing is recommended as it yields the highest flexural modulus and strength and is better suited to large-scale (industrial) nanocomposite fabrication than US mixing. The largest flexural modulus is achieved at a VGCNF weight fraction $D = 0.48$ phr. The greatest flexural strength is observed at $D = 0.60$ phr of VGCNF. So, a nanofiber weight fraction $D \approx 0.50$ phr is recommended for optimal VGCNF/VE flexural properties. The results of this work augment those of a previous study of the dynamic mechanical analysis of the same nanocomposite system,[24] where a roughly 20% increase in the storage modulus was observed with the addition of VGCNFs to VE at 0.37–0.54 phr.

Lastly, if the combination of factorial levels is not optimal, then this can lead to *lower* flexural moduli and strengths as well as significantly *more scatter* in the data. For example, nanocomposites prepared with pristine VGCNFs and DA [E_2 in Figure 3(b)] displayed relatively low flexural moduli and a high degree of scatter over the range of nanofiber weight fractions considered. In contrast, nanocomposites prepared with oxidized nanofibers and DA using high shear mixing showed the highest

moduli over the same range. Equally important, the latter nanocomposites showed the *least* amount of scatter in the data. Hence, the factor level combination that leads to the greatest flexural moduli also minimizes the scatter in the experimental data. Similar arguments can be made regarding optimizing nanocomposite strengths.

SUMMARY AND CONCLUSIONS

A statistical design of experiments was performed to investigate the effects of formulation and processing factors, i.e., (1) VGCNF type, (2) use of a dispersing agent (DA), (3) mixing method (ultrasonication, high-shear mixing, and a combination of both), and (4) VGCNF weight fraction, on the flexural moduli and strengths of VGCNF/VE nanocomposites. This powerful statistical tool in conjunction with response surface modeling enables tailoring of nanocomposite systems and prediction of material performance and mechanical characteristics based on desired application goals. In this article, the flexural modulus was sensitive to a set of complex two-factor interactions among the four factors. The highest flexural modulus was obtained where oxidized VGCNFs, DA, and high-shear mixing were used at 0.48 phr of VGCNF. This tiny amount of nanofibers resulted in a 19% increase in the flexural modulus over that of the neat VE. The flexural strength was sensitive to several two-factor interactions. The highest flexural strength was obtained for the case where high-shear mixing was used at $D = 0.60$ phr of VGCNF. This very small amount of nanofibers gave a 49% increase in the flexural strength over that of the neat VE. For this case, the VGCNF type and use of a DA did not significantly affect the mean flexural strength. The use of oxidized VGCNFs, DA, and high-shear mixing at a VGCNF weight fraction $D \approx 0.50$ phr is recommended to optimize both flexural modulus and strength of VGCNF/VE nanocomposites within the design space of this article. While these results are restricted to the VGCNF/VE system and the processing methods considered here, RSMs similar to those developed in this article may be used to characterize the behavior of thermosetting or thermoplastic polymers containing nanoparticles with varying sizes, shapes, composition, and weight fractions. Such approaches may be used to tailor nanocomposite properties over a range of operating environments, provide insight into relevant physical behavior, as well as guide the development of physics-based models.

ACKNOWLEDGMENTS

This work was sponsored by the U. S. Department of Energy under contract DE-FC26-06NT42755. Special thanks go to William Joost, Department of Energy's technology area development manager.

APPENDIX

In this appendix, the treatment combinations and their responses are given in Table AI. Tables AII and AIII provide parameter

Table AI. Treatment Combinations and their Average Responses[a] Presented in the ascending order of VGCNF Weight Fractions at Fixed Levels of the Factors. The run Numbers Indicate the Actual Order of Conducting the Experiments after Randomizing the Treatment Combinations to Eliminate Bias

Run	A: VGCNF type	B:Use of a dispersing agent	C: Mixing method	D: VGCNF Weight fraction (phr)	Flexural modulus (GPa)	Flexural strength (MPa)
52	Pristine	No	US[b]	0.00	3.11	67.6
4	Pristine	No	US	0.25	3.02	47.6
7	Pristine	No	US	0.50	3.11	45.3
23	Pristine	No	US	0.75	3.27	53.5
17	Pristine	No	US	1.00	2.93	49.7
24	Pristine	No	HS[c]	0.00	3.11	67.6
22	Pristine	No	HS	0.25	3.08	97.7
20	Pristine	No	HS	0.50	3.15	104.8
9	Pristine	No	HS	0.75	3.43	89.1
15	Pristine	No	HS	1.00	3.29	79.2
46	Pristine	No	HS/US[d]	0.00	3.11	67.6
47	Pristine	No	HS/US	0.25	2.88	112.1
48	Pristine	No	HS/US	0.50	3.18	79.5
8	Pristine	No	HS/US	0.75	3.32	117.1
2	Pristine	No	HS/US	1.00	3.16	87.7
57	Pristine	Yes	US	0.00	3.11	67.6
60	Pristine	Yes	US	0.25	3.44	50.4
6	Pristine	Yes	US	0.50	3.37	82.2
54	Pristine	Yes	US	0.75	3.24	88.4
53	Pristine	Yes	US	1.00	3.22	96.9

TABLE AI. *Continued*

Run	A: VGCNF type	B:Use of a dispersing agent	C: Mixing method	D: VGCNF Weight fraction (phr)	Flexural modulus (GPa)	Flexural strength (MPa)
50	Pristine	Yes	HS	0.00	3.11	67.6
25	Pristine	Yes	HS	0.25	3.36	103.5
34	Pristine	Yes	HS	0.50	3.20	105.0
13	Pristine	Yes	HS	0.75	3.34	104.8
3	Pristine	Yes	HS	1.00	3.39	96.1
37	Pristine	Yes	HS/US	0.00	3.11	67.6
42	Pristine	Yes	HS/US	0.25	3.51	77.5
36	Pristine	Yes	HS/US	0.50	2.99	80.9
10	Pristine	Yes	HS/US	0.75	3.18	82.3
27	Pristine	Yes	HS/US	1.00	3.15	83.1
49	Oxidized	No	US	0.00	3.11	67.6
19	Oxidized	No	US	0.25	2.59	39.0
21	Oxidized	No	US	0.50	2.86	58.9
18	Oxidized	No	US	0.75	2.98	64.4
59	Oxidized	No	US	1.00	3.06	45.7
29	Oxidized	No	HS	0.00	3.11	67.6
33	Oxidized	No	HS	0.25	3.34	85.5
28	Oxidized	No	HS	0.50	3.53	85.7
35	Oxidized	No	HS	0.75	3.57	96.4
40	Oxidized	No	HS	1.00	3.64	85.5
32	Oxidized	No	HS/US	0.00	3.11	67.6
56	Oxidized	No	HS/US	0.25	3.02	80.9
12	Oxidized	No	HS/US	0.50	3.07	81.2
30	Oxidized	No	HS/US	0.75	3.36	82.7
14	Oxidized	No	HS/US	1.00	3.55	102.6
44	Oxidized	Yes	US	0.00	3.11	67.6
16	Oxidized	Yes	US	0.25	2.86	38.1
1	Oxidized	Yes	US	0.50	2.95	67.2
51	Oxidized	Yes	US	0.75	2.94	97.3
39	Oxidized	Yes	US	1.00	3.59	66.4
43	Oxidized	Yes	HS	0.00	3.11	67.6
5	Oxidized	Yes	HS	0.25	3.65	89.6
26	Oxidized	Yes	HS	0.50	3.63	104.3
11	Oxidized	Yes	HS	0.75	3.69	87.9
55	Oxidized	Yes	HS	1.00	3.61	92.4
41	Oxidized	Yes	HS/US	0.00	3.11	67.6
58	Oxidized	Yes	HS/US	0.25	2.94	71.9
31	Oxidized	Yes	HS/US	0.50	3.09	82.2
38	Oxidized	Yes	HS/US	0.75	3.28	77.6
45	Oxidized	Yes	HS/US	1.00	3.30	108.2

[a] The average value of two independent samples was used to obtain the responses. The standard deviations for the storage modulus data were in the range 100–200 MPa and for the loss modulus data were in the range 5–10 MPa.

[b] Ultrasonication.

[c] High-shear mixing.

[d] Coupled high-shear mixing and ultrasonication.

Note: The treatment combinations involving 0.00 phr VGCNF are simply neat resin specimens all prepared the same way irrespective of the other factor levels.

Table AII. Regression Analysis Results Pertaining to Response Surface Models E_1, E_2, E_3, and E_4 for the Flexural Modulus

Parameter	Degrees of freedom	Parameter estimate	Standard error	*t*-value	*P*-value
E_1 (pristine VGCNF without dispersing agent)					
Intercept (β_0)	1	3.12	0.057	54.53	<0.0001
β_1	1	−1.63	0.58	−2.80	0.0172
β_2	1	5.26	1.48	3.57	0.0044
β_3	1	−3.62	0.97	−3.73	0.0033
R^2: 0.63, adjusted R^2: 0.53					
Max flexural modulus = 3.33 GPa at D = 0.78 phr					
E_2 (pristine VGCNF with dispersing agent)					
Intercept (β_0)	1	3.13	0.076	41.03	<0.0001
β_1	1	1.86	0.78	2.40	0.0353
β_2	1	−4.42	1.97	−2.24	0.0465
β_3	1	2.70	1.30	2.08	0.0614
R^2: 0.34, adjusted R^2: 0.17					
Max flexural modulus = 3.36 GPa at D = 0.29 phr					
E_3 (oxidized VGCNF with high-shear mixing and no dispersing agent)					
Intercept (β_0)	1	3.11	0.031	98.84	0.0064
β_1	1	1.27	0.32	3.97	0.1572
β_2	1	−1.17	0.81	−1.44	0.3864
β_3	1	0.43	0.53	0.81	0.5671
R^2: 0.99, adjusted R^2: 0.98					
Max flexural modulus = 3.64 GPa at D = 1.00 phr					
E_4 (oxidized VGCNF with high-shear mixing and dispersing agent)					
Intercept (β_0)	1	3.12	0.099	31.60	0.0201
β_1	1	2.95	1.01	2.93	0.2093
β_2	1	−4.70	2.55	−1.84	0.3167
β_3	1	2.26	1.68	1.34	0.4073
R^2: 0.96, adjusted R^2: 0.83					
Max flexural modulus = 3.71 GPa at D = 0.48 phr					

Table AIII. Regression Analysis Results Pertaining to Response Surface Models S_1, S_2, S_3, and S_4 for the Flexural Strength

Parameter	Degrees of freedom	Parameter estimate	Standard error	*t*-value	*P*-value
S_1 (ultrasonication without dispersing agent)					
Intercept (β_0)	1	67.3	4.1	16.3	<0.0001
β_1	1	−183.9	42.1	−4.4	0.0047
β_2	1	437.0	106.9	4.1	0.0065
β_3	1	−273.0	70.3	−3.9	0.0081
R^2: 0.78, adjusted R^2: 0.66					
Max flexural strength = 60.2 MPa at D = 0.78 phr					
S_2 (ultrasonication with dispersing agent)					
Intercept (β_0)	1	66.9	7.9	8.4	0.0002
β_1	1	−221.3	80.7	−2.7	0.0337
β_2	1	678.8	205.0	3.3	0.0162
β_3	1	−443.4	134.7	−3.3	0.0166
R^2: 0.77, adjusted R^2: 0.66					
Max flexural strength = 97.4 MPa at D = 0.82 phr					
S_3 (high-shear mixing)					
Intercept (β_0)	1	69.5	3.6	19.5	<0.0001
β_1	1	104.6	16.9	6.2	<0.0001
β_2	1	−87.8	16.2	−5.4	<0.0001
R^2: 0.71, adjusted R^2: 0.68					
Max flexural strength = 100.6 MPa at D = 0.60 phr					
S_4 (coupled high-shear mixing/ultrasonication)					
Intercept (β_0)	1	68.3	6.3	10.9	<0.0001
β_1	1	92.2	64.0	1.4	0.1692
β_2	1	−166.8	162.6	−1.0	0.3201
β_3	1	102.5	106.9	1.0	0.3517
R^2: 0.39, adjusted R^2: 0.27					
Max flexural strength = 96.2 MPa at D = 1.00 phr					

estimates and their statistics for to the flexural modulus and flexural strength RSMs, respectively.

REFERENCES

1. Koo, J. H. Polymer Nanocomposites: Processing, Characterization, and Applications; McGraw-Hill: New York, NY, **2006**.
2. Kotsilkova, R.; Pissis, P. Thermoset Nanocomposites for Engineering Applications; Smithers Rapra Technology: Shropshire, UK, **2007**.
3. Mittal, V. Optimization of Polymer Nanocomposite Properties; Wiley-VCH: Weinheim, Germany, **2010**.
4. Thostenson, E. T.; Li, C.; Chou, T. W. *Compos. Sci. Technol.* **2005**, *65*, 491.
5. Wagner, H. D.; Vaia, R. A. *Mater. Today* **2004**, *7*, 38.
6. Jordan, J.; Jacob, K. I.; Tannenbaum, R.; Sharaf, M. A.; Jasiuk, I. *Mater. Sci. Eng. A* **2005**, *393*, 1.
7. Gibson, R. F.; Ayorinde, E. O.; Wen, Y. F. *Compos. Sci. Technol.* **2007**, *67*, 1.
8. Tibbetts, G. G.; McHugh, J. J. *J. Mater. Res.* **1999**, *14*, 2871.
9. Thostenson, E. T.; Ziaee, S.; Chou, T. W. *Compos. Sci. Technol.* **2009**, *69*, 801.
10. Faraz, M. I.; Bhowmik, S.; De Ruijter, C.; Laoutid, F.; Benedictus, R.; Dubois, P.; Page, J. V. S.; Jeson, S. *J. Appl. Polym. Sci.* **2010**, *117*, 2159.
11. Jimenez, G. A.; Jana, S. C. *Compos. Part A Appl. S.* **2007**, *38*, 983.
12. Lozano, K.; Barrera, E. V. *J. Appl. Polym. Sci.* **2001**, *79*, 125.
13. Liao, Y. H.; Marietta-Tondin, O.; Liang, Z.; Zhang, C.; Wang, B. *Mater. Sci. Eng. A* **2004**, *385*, 175.
14. Zhang, W.; Joshi, A.; Wang, Z.; Kane, R. S.; Koratkar, N. *Nanotechnology* **2007**, *18*, 185703.
15. Cho, J.; Daniel, I. M.; Dikin, D. A. *Compos. Part A Appl. S.* **2008**, *39*, 1844.

16. Rasheed, A.; Dadmun, M. D.; Britt, P. F. *J. Polym. Sci. Part B Polym. Phys.* **2006**, *44*, 3053.
17. Lakshminarayanan, P. V.; Toghiani, H.; Pittman, C. U., Jr *Carbon* **2004**, *42*, 2433.
18. Tibbetts, G. G.; Lake, M. L.; Strong, K. L.; Rice, B. P. *Compos. Sci. Technol.* **2007**, *67*, 1709.
19. Goodman, S. H. Handbook of Thermoset Plastics; Noyes Publications: Westwood, NJ, **1998**.
20. McConnell, V. P. *Reinf. Plast.* November/December 2010 issue, *54*, 34.
21. Plaseied, A.; Fatemi, A.; Coleman, M. R. *Polym. Polym. Compos.* **2008**, *16*, 405.
22. Plaseied, A.; Fatemi, A. *J. Reinf. Plast. Compos.* **2009**, *28*, 1775.
23. Hutchins, J. W.; Sisti, J.; Lacy, T. E., Jr.; Nouranian, S.; Toghiani, H.; Pittman, C. U., Jr. 50th AIAA/ASME/ASCE/AHS/ASC Structures, Structural Dynamics and Materials Conference, Palm Springs, CA, **2009**.
24. Nouranian, S.; Toghiani, H.; Lacy, T. E.; Pittman, C. U.; Dubien, J. *J. Compos. Mater.* **2011**, *45*, 1647.
25. Nouranian, S.; Lacy, T. E.; Toghiani, H.; Pittman Jr, C. U.; Dubien, J. L. *J. Appl. Polym. Sci.* **2013**, DOI: 10.1002/app.39041.
26. Torres, G. W.; Nouranian, S.; Lacy, T. E.; Toghiani, H.; Pittman, C. U., Jr.; Dubien, J. *J. Appl. Polym. Sci.* **2013**, *128*, 1070.
27. Cox, D. R.; Reid, N. The Theory of the Design of Experiments; Chapman & Hall/CRC: Boca Raton, FL, **2000**.
28. Myers, R. H.; Montgomery, D. C.; Anderson-Cook, C. M. Response Surface Methodology: Process and Product Optimization using Designed Experiments; John Wiley & Sons: Hoboken, NJ, **2009**.
29. Lacy, T. E.; Samarah, I. K.; Tomblin, J. S. *SAE Int. J. Aerosp.* **2002**, 126.
30. Yong, V.; Hahn, H. T. *Nanotechnology* **2005**, *16*, 354.
31. Samarah, I. K.; Weheba, G. S.; Lacy, T. E. *SAE Int. J. Aerosp.* **2006**, 767
32. Samarah, I. K.; Weheba, G. S.; Lacy, T. E. *J. Appl. Stat.* **2006**, *33*, 429.
33. Chow, W.; Yap, Y. *Express. Polym. Lett.* **2008**, *2*, 2.
34. Li, H. Synthesis, characterization, and properties of vinyl ester matrix resins. PhD Dissertation Thesis, Virginia Polytechnic Institute and State University, Blacksburg, VA USA, **1998**.
35. Jang, C. Nouranian, S.; Lacy, T. E.; Gwaltney, S. R.; Toghiani, H.; Pittman, C. U., Jr. *Carbon* **2012**, *50*, 748.
36. Ellison, S. L. R.; Barwick, V.; Farrant, T. J. Practical Statistics for the Analytical Scientist: A Bench Guide; The Royal Society of Chemistry Publishing: Cambridge, UK, **2009**.
37. Brown, M. B. *Appl. Stat.* **1975**, *24*, 288.
38. Montgomery, D. C. Design and Analysis of Experiments; Wiley: Hoboken, NJ, **2009**.
39. Fu, Y.; Han, C.; Ni, Q. *Chin. J. Chem* . **2009**, *27*, 1110.
40. Sudduth, R. D. *Pigment Resin Technol.* **2008**, *37*, 362.
41. Yu, J.; Lacy, T. E.; Toghiani, H.; Pittman, C. U., Jr. *J. Compos. Mater.* **2011**, *45*, 2401.
42. Dzenis, Y. A. *Science* **2008**, *319*, 419.